

Growth of Epitaxial ZnS, ZnSe and ZnS-ZnSe Multilayers on GaAs by Pulsed-Laser Ablation

J. W. McCamy*, Douglas H. Lowndes†, and J.D. Budai†

* Department of Materials Science and Engineering, The University of Tennessee, Knoxville, TN 37996-1200

† Solid State Division, Oak Ridge National Laboratory, Oak Ridge, TN 37831-6056

Pulsed KrF (248nm) laser ablation of polycrystalline ZnS and ZnSe targets has been used to grow high quality, carbon-free, fully epitaxial ZnS and ZnSe thin films on GaAs (001) and GaAs (111). The films were grown using a deposition geometry that produces highly uniform thickness. By alternately ablating each target, strained layer superlattices of the form $(\text{ZnSe})_m(\text{ZnS})_n$ and $(\text{ZnSe})_m(\text{ZnS}_x\text{Se}_{1-x})_n$, having as many as 65 periods, were grown. Period widths ranged from $\sim 50\text{\AA}$ to 350\AA .

1. INTRODUCTION

Zinc sulfide (ZnS) and zinc selenide (ZnSe) are attractive thin-film optoelectronic materials because of their wide direct bandgaps ($E_g = 3.7\text{ eV}$ and $E_g = 2.7\text{ eV}$, respectively). Potential applications for these materials include optically bistable switching devices for information processing, optical waveguides, and blue LEDs or laser diodes. The techniques most often used to grow ZnS and ZnSe thin films include physical transport methods (e.g., elemental vapor transport) and metalorganic chemical vapor deposition (MOCVD). However, the physical transport methods require high growth temperatures of $500\text{--}900^\circ\text{C}$; defect complexes, which may act as carrier trapping centers, are formed at these temperatures. Experience to date with MOCVD shows that the principal problems are either premature reactions when hydride-zinc alkyl systems (e.g., H_2S and diethylzinc) are used, or the high temperatures needed to promote many alkyl-alkyl reactions (e.g., dimethylzinc and dimethylsulfur).¹⁾ In recent years, growth of these materials by molecular beam epitaxy has met with some success in overcoming these difficulties.²⁾

Pulsed-laser ablation (PLA) is an attractive alternative deposition method that uses solid, carbon-free sources. While PLA has become widely known recently for growth of epitaxial high-temperature superconductor films, it also can be used to grow epitaxial films of other ceramics,³⁾ as well as semiconductors.^{4), 5)} PLA has several fundamental advantages, including stoichiometric transport of material from the ablation target to the substrate surface, when the laser beam conditions are correctly adjusted; growth of smooth films when the laser

energy density, E_d , and the target surface morphology are controlled properly; and, the ability to grade compositionally an epitaxial layer.⁶⁾ Like the MBE growth technique, PLA has the potential to grow films with submonolayer precision. Additionally, with PLA the film composition can be changed readily simply by exchanging targets, which allows strained-layer superlattices (SLS) of two or more materials to be grown easily.⁷⁾ Another characteristic of PLA film deposition is that the angular distribution of ablated material usually is strongly peaked in the forward direction ($\sim [\cos \Theta]^n$, with $n \sim 1.5\text{--}10$)^{8), 9)}, so that the film thickness varies rapidly with position.

2. EXPERIMENTAL

GaAs(001) and GaAs(111) substrates were degreased in organic solvents, then etched (15 s) in concentrated H_2SO_4 . The substrate surfaces then were passivated in an $(\text{NH}_4)_2\text{S}_x$ solution, mounted on the substrate heater, and introduced into the growth chamber (2×10^{-7} Torr base pressure). Immediately before film growth, the substrates were heated to 420°C for 3 minutes, then cooled to the growth temperature.

The substrate heater was designed with a pumped (double O-ring) seal to allow the substrate-target separation to be varied while still permitting substrate rotation during growth. The target and substrate faces were vertical and parallel, with coincident rotational centerlines. The substrate-target separation, D_{st} , was maintained at 10.8 cm. Growth was carried out in a 2 mTorr atmosphere of ultra-high purity (99.9999+ %) helium. Earlier work showed

that growth in this ambient had no effect on film quality.¹⁰⁾

A pulsed KrF (248nm) excimer laser beam (~35 ns FWHM pulse duration) was passed through an aperture and brought to a vertical focus on a 2.54 cm-diam polycrystalline ZnS or ZnSe target (Angstrom Sciences, 99.999+ % purity) using a single +50 cm cylindrical lens. The data reported here were obtained using $E_L = 0.35 \text{ J/cm}^2$. The laser beam was incident on the target at an angle of $\sim 25^\circ$ from the surface normal, with a horizontal offset $L = 0.5\text{--}0.7 \text{ cm}$ from the rotational centerline. The laser repetition rate was 1 Hz, corresponding to 12.5 laser pulses per substrate revolution. The combination of beam offset and substrate rotation exploits the strongly forward-peaked ablation distribution. For $D_{st} = 5.7 \text{ cm}$ films are completely uniform ($< \pm 1\%$) in thickness over areas of $\sim 75 \text{ mm}^2$, with good thickness uniformity ($< \pm 3\%$) over areas of $\sim 300 \text{ mm}^2$.¹⁰⁾ By modeling the film thickness uniformity as a function of D_{st} and L , we found that film thickness uniformity can be achieved over much larger areas simply by scaling, i.e., using larger separations and offsets. Thus, although the small size of the ablation target and chamber were constraining factors in this work, these are not fundamental constraints on larger-scale semiconductor-growth applications of the PLA method.

The chamber was equipped with a multitarget holder which allowed *in-situ* substitution of ablation targets; by simply alternating targets, thin film multilayers were grown. The film-growth rate was monitored *in-situ* from interference oscillations in the intensity of a HeNe (633 nm) laser beam reflected from the upper and lower surfaces of the growing film. For the growth conditions given here, typical growth rates were determined to be $\sim 2 \text{ \AA}$ per laser pulse for growth along the (001) direction. For growth along (111) typical growth rates were $\sim 1.5 \text{ \AA}$ per laser pulse. Thus, the possibility of sub-unit cell control of the multilayer interfaces was achieved. Before a multilayer was grown, an epitaxial ZnSe, $\text{ZnS}_{0.06}\text{Se}_{0.94}$, or $\text{ZnS}_{0.11}\text{Se}_{0.89}$ buffer layer, of 1500–3500 \AA thickness, was deposited. Following growth of the multilayer a capping layer $\sim 200 \text{ \AA}$ thick, and having the same composition as the buffer layer, was deposited. Multilayers consisted either of alternating ZnSe–ZnS, ZnSe– $\text{ZnS}_{0.16}\text{Se}_{0.84}$, or $\text{ZnS}_{0.12}\text{Se}_{0.88}$ – $\text{ZnS}_{0.06}\text{Se}_{0.94}$ layers. As many as 65 periods (130 layers), ranging in thickness from 50 \AA to 360 \AA , were grown. In all cases the ratio of the layer thicknesses ($t_1 : t_2$) was 2 : 1, chosen so that the intensity of the even superlattice x-ray diffraction (XRD) peaks would be enhanced.¹¹⁾

Room temperature photoluminescence (PL) measurements of the ZnS and ZnSe films were performed using a pulsed KrF (248 nm, 29 ns FWHM pulse duration) excimer laser as the excitation source. The intensity was reduced using

beam splitters such that the incident energy density ranged between 1.0 – 2.5 mJ/cm^2 (35–85 kw/cm^2 .) The spectra were measured using a McPherson 1.3 m spectrometer. A boxcar integrator was used to process the PMT signal; errors in counting statistics were further reduced by averaging readings from multiple excitations (typically ~ 10 .) The center of the boxcar gate was set at 40 ns following the arrival of the excitation pulse and had a width of 80 ns. Low temperature ($\sim 9 \text{ K}$) PL measurements currently are being performed.¹²⁾

3. RESULTS

The crystal structure and epitaxial orientation of the films were characterized by Cu $K\alpha$ XRD. For growth on GaAs(001), both the ZnS[001] and ZnSe[001] were aligned to within $< 0.2^\circ$ of the GaAs[001], and that the in-plane [100] and [010] directions of both films were aligned with the respective directions of the underlying GaAs substrates. Thus, growth of ZnS and ZnSe on GaAs(001) was fully epitaxial.

To determine the optimum growth temperature, ZnS and ZnSe films were grown to a thickness of $\sim 2500 \text{ \AA}$ for the film-growth temperature range $T_g = 150\text{--}450^\circ\text{C}$ and the XRD rocking curve width (FWHM) of the (004) peak was measured. At all growth temperatures two superimposed peaks, one narrow (\sim limit of resolution) and one much broader ($> 0.4^\circ$), were seen in the ZnS(004) rocking curve line profiles. These are characteristic of diffraction from films that contain regions of near-perfect and regions of strained (or otherwise defective) crystalline material. Both high resolution TEM and RBS confirm the presence of a strained/defective layer at the ZnS–GaAs interface.¹⁰⁾ The ZnSe(004) rocking curve profiles from samples grown at temperatures of 300°C and greater showed only a single, narrow peak, indicating little or no strained material in the films grown under these conditions. For ZnSe films grown at temperatures less than 300°C , however, two superimposed peaks (similar to the ZnS response) were observed, indicating the presence of strained material.

For ZnS on GaAs, the rocking curve width reached a minimum at $\sim 325^\circ\text{C}$. However, the width of the ZnSe rocking curve declined continuously as the temperature was decreased, reaching a minimum at 300°C ; as noted above, strained material was observed at this point. From this, we conclude that the optimum temperature for ZnS on GaAs is 325°C , and $\sim 300^\circ\text{C}$ for ZnSe.

Figure 1 shows the θ - 2θ XRD pattern for a ZnSe–ZnS multilayer grown on GaAs(001) at $T_g = 325^\circ\text{C}$. The multilayer structure consisted of 65 periods (20 shots ZnSe, 10 shots ZnS, with 1.67 \AA per shot measured *in-situ*), grown on a 3700 \AA thick ZnSe buffer layer, and capped with a 170 \AA ZnSe layer. Superlattice satellite peaks are easily seen; the

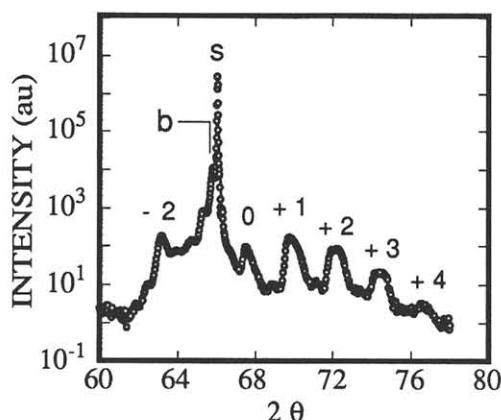


Figure 1. X-ray diffraction pattern (θ - 2θ) for a 65 period ZnSe-ZnS SLS grown on (001) GaAs at $T_g = 325^\circ\text{C}$.

spacing of these peaks indicates the period of the SL is 48 Å, which compares well with the value calculated from the *in-situ* growth rate measurement. The calculated lattice constant parallel to the surface normal for a SLS with this structure is 5.56 Å ($2\theta = 67.3^\circ$), which is in agreement with the zeroth peak assignment shown ($2\theta = 67.54^\circ$). The other peak assignments were made by approximating the superlattice as a $(\text{ZnSe})_6$ - $(\text{ZnS})_3$ structure, and calculating a simple pattern using kinematical XRD theory.

Both the ZnS and ZnSe films showed strong near-bandedge (NBE) room temperature PL emission. The peak maximum (I_{max}) of the NBE for the ZnS samples was found at $E_{\text{lum}} = 3.69$ eV (see Figure 2); the "shoulder" (Figure 2 insert) at $E_{\text{lum}} = 3.65$ eV was consistently seen in all the ZnS samples. For undoped ZnS films, the as-measured NBE peak width was ~80 meV.

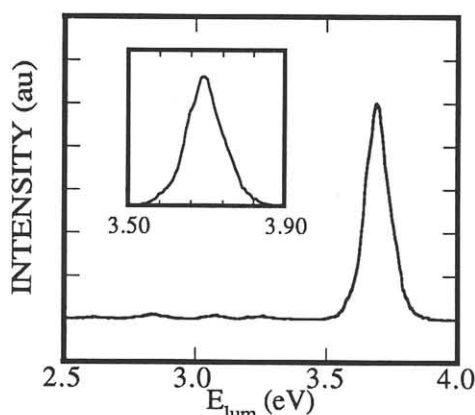


Figure 2. Room temperature photoluminescence spectrum for an undoped ZnS thin film (~3000 Å).

For the ZnSe thin films, I_{max} was found at $E_{\text{lum}} = 2.71$ eV; the as-measured ZnSe NBE peak width was ~45 meV. Preliminary low temperature PL results indicate that the NBE in both cases is dominated by free excitons and donor-bound excitons.¹²⁾ In the ZnS room temperature PL spectra deep center emission peaks also were observed. These are being studied further using low-temperature PL.

4. CONCLUSIONS

In summary, we have demonstrated that PLA is an attractive method for growth of fully epitaxial ZnS and ZnSe thin films with excellent thickness uniformity. These PLA-grown films have the advantage that they are inherently carbon-free. Control of the PLA growth process is such that high quality SLS of these materials can be fabricated easily.

This research was sponsored by the Division of Materials Sciences, U.S. Department of Energy under contract DE-AC05-84OR21400 with Martin Marietta Energy Systems, Inc.

REFERENCES

- 1) H. Kukimoto, *J. Cryst. Growth* **107**(1991) 637.
- 2) D.L. Dreifus, B.P. Sneed, J. Ren, J.W. Cook, J.F. Schetzina, *Appl. Phys. Lett.*, **57**, (1990) 1663
- 3) L. Shi, H. J. Frankena, *Vacuum* **40**(1990) 399.
- 4) D. Lubben, S. A. Barnett, K. Suzuki, S. Gorbatskin, J. E. Greene, *J. Vac. Sci. Technol. B.* **3**(1985) 968.
- 5) J. J. Dubowski, *Chemitronics* **3**(1988) 66.
- 6) J. T. Cheung, E. H. Cirilin, N. Otsuka, *Appl. Phys. Lett.* **53**(1988) 310.
- 7) J.J. Dubowski, J.R. Thompson, S.J. Rolfe, J.P. McCaffrey, *Superlattices and Microrstructures* **9**(1991) 327
- 8) T. Venkatesan, X. D. Wu, A. Inam, J. B. Wachtman, *Appl. Phys. Lett.* **52**(1988) 1193
- 9) R. E. Muenchausen, K. M. Hubbard, S. Foltyn, R. C. Estler, and N. S. Nogar, *Appl. Phys. Lett.* **56**(1990).578
- 10) J.W. McCamy, D.H. Lowndes, J.D. Budai, R.A. Zuhr, X. Zhang, *Appl. Phys. Lett.*, to be published
- 11) A. Appel, U. Bonse, J. Staudenmann, *Z. Phys. B.*, **81**(1990) 371
- 12) J.W. McCamy, D.H. Lowndes, I. Herman, S.Kim, unpublished